Turkish Journal of Agriculture - Food Science and Technology, 10(12): 2446-2452, 2022
DOI: https://doi.org/10.24925/turjaf.v10i12.2446-2452.5535

Turkish Journal of Agriculture - Food Science and Technology

Available online, ISSN: 2148-127X | www.agrifoodscience.com | Turkish Science and Technology Publishing (TURSTEP)

Evaluation from Rural to Urban Scale for the Effect of NDVI-NDBI Indices on Land Surface Temperature, in Samsun, Türkiye

Burcu Çevik Değerli[1,a,*] Mehmet Çetin[2,b]

[1]*Department of Landscape Architecture, Institute of Science, Kastamonu University, 37200 Kastamonu, Türkiye*
[2]*Department of City and Regional Planning, Faculty of Architecture, Ondokuz Mayis University, 55200 Samsun, Türkiye*
[*]*Corresponding author*

A R T I C L E I N F O

Research Article

Received : 25/09/2022
Accepted : 31/10/2022

Keywords:
Land Surface temperature (LST)
Vegetation index (NDVI)
Structuring index (NDBI)
Urban Scale
Samsun

A B S T R A C T

In this study, in order to evaluate the change of LST from rural to urban scale in 20 years, a zoonal statistical analysis was performed by separating the urban and rural districts located on the coastline. Algorithms were applied to the raw data of Landsat 8 and Landsat 7 satellite images, using the Arc Gis 10.2 and Q Gis 3.16 utilities. In this way, NDVI, NDBI and LST data were compared and evaluated in terms of rural and urban districts. The correlation coefficient between the parameters was calculated. In the study, the land change between the years 2000-2020 was also determined to reveal the land change. As a result of the analyzes made, the amount of green areas decreased by 14.1% between 2000 and 2020 in the study area, which includes the central districts of Samsun, İlkadım and Atakum, and in the rural areas, Bafra and Ondokuz Mayıs. It has been observed that this rate is shared as 7.1% in built up areas and 7.33% in bare soil areas. Considering the effect of the decrease in green areas on the LST value, in 2000, max. While LST is 41.75 C, in 2020 max. It is seen that LST has increased to 43.44 C. When the districts were analyzed separately, it was seen that LST established a strong correlation with NDBI (positive) and NDVI (negative) for all four districts. However, the correlation was stronger in rural districts. It was observed that the correlation strength weakened in urban districts due to heterogeneous land surface cover.

[a] burcu.degerli@omu.edu.tr https://orcid.org/0000-0001-5152-6406 | [b] mehmet.cetin@omu.edu.tr https://orcid.org/0000-0002-8992-0289

Introduction

Overheating of cities has negative consequences on people's living comfort and energy consumption. Cities are the areas where climate change is felt the most. (Oke, 1982). Cities create local climatic zones and create a kind of microclimate area. Cities are on average 4°C warmer than the surrounding countryside (Oleson et al. 2011). Decrease in vegetation and evaporation surfaces in cities, increase in impermeable surfaces, overheating of surface coating materials used in urban design as a result of trapping sunlight; It negatively affects the topography, ecological structure, and atmospheric and climatic characteristics of the city (Çelik, 2019).

Samsun has undergone radical changes in the last 50 years as a result of the settlement pressure concentrated on the coastal areas due to urbanization, population growth and socio-economic developments (SBB, 2014). After 1998, the urban settlement area in Samsun increased by 96.32% and grew to approximately 32 km², and this growth generally developed towards agricultural areas. Atakum district has become a second city center since 1998 (Ozturk, 2017). Atakum has the highest population growth in Samsun Province (SBB, 2014; TÜİK, 2020). The average annual growth rate of the district is around 63.5% and there is a significant immigrant population from other districts and other provinces in Samsun. (AK, 2013). The city is witnessing rapid urbanization trends that facilitate vegetation loss in the region.

One of the major and visible anthropogenic land use changes in modern times is the urbanization of rural areas (Roth, 2007). In the urbanization process, the land loses its vegetation and turns into impermeable surfaces. Changes in anthropogenic land use affect regional and global climate (Change, 2019, Pielke Sr, 2005). When examining urban climatic phenomena, the uniform physical characteristics of cities may weaken the examination of rural-urban differences in climatic conditions. Therefore, it is important to include rural areas in the study area to avoid bias (Roth, 2007). For Samsun province, studies in the literature about its climate and change is the researchers mentioned about Samsun climate changed effectively (Basci and Bahadır, 2019; Guler et al., 2007; Karabulut et al., 2008; Ülke and Özkoca, 2018)

The common approach used in these studies is to investigate the effect of the temporal changes of average monthly, annual, seasonal air temperature, precipitation, humidity on climate change. One of these studies, Başci and Bahadır (2019) studied the temporal change of land cover in the fertile Kızılırmak Delta by working on the rural scale of Bafra from satellite images. Today, there are many studies on global and regional climate changes in the literature. In our study, the effect of NDVI and NDBI on LST and the effect of increasing LST on climate change were investigated. In order to deal with climate change in the dimension of urban planning, it was decided that NDVI, NDBI change and LST should be correlated, except for meteorological data. Surface-based solutions can help reduce and adapt to climate change by lowering air temperature.

Based on these predictions in the study, the questions of interest of the study were determined as follows:

- What is the quantitative change in LC/LU between 2000-2020?
- What is the temporal variation of LST?
- What is the temporal change in the NDVI index and how did this change affect the LST?
- What is the temporal change in the NDBI index and how did this change affect the LST?
- How is the correlation between LST and NDVI, NDBI affected when we separate the urban and rural districts in the study area?

Remote sensing and statistical methods were used to find answers to these questions. In the study, Landsat 7 and Landsat 8 data were processed using Q Gis 3.16 and ArcGis 10.5 programs and machine learning algorithms.

Materials and Methods

Samsun province, located in the middle of the Black Sea coastline, between the Kızılırmak and Yeşilırmak rivers flowing into the Black Sea, has an area of 9,725 km² (Figure 1). Samsun province has three different features in terms of landforms. The first is mountainous in the south, the second is the plateaus between the mountainous coastline and the coastline, and the third is the coastal plain between the Black Sea. Streams in the region have largely fragmented the land between the plateaus. The geographical location of the study area is between 40° 50' - 41° 51' north latitudes, 37° 08' and 34° 25' east longitudes. The altitude of Samsun is approximately 4.00 m (Sitom, 2007). Samsun generally has a mild climate. The climate has two distinct features in the coastline and inland. The effects of the Black Sea climate are seen on the coastline. On the coasts, summers are hot, winters are warm and rainy, while the inner parts are under the influence of 2000 meters high Akdağ and 1500 meters high Canik Mountains. As a result of this effect of the mountains, the winter season is cold, rainy and snowy, and the summer season is cool. Average annual precipitation totals are 707.21mm above the national average. The biggest rivers of the province are Kızılırmak and Yeşilırmak. These two rivers cross the provincial territory and reach the Black Sea (SKTM, 2020).

Data Sources and Programs

Landsat 7 ETM+ (Collection 1, level 1), Landsat 8 OLI/TIRS (Collection 1, Level 1) satellite images were obtained from the United States Geological Survey site (USGS, 2020). The satellite images used are shown in Table 1. GIS and Image processing software platform ArcGIS 10.5, QGis 3.16 programs were used for preprocessing of satellite data, application of algorithms and spatial analysis. SPSS 24 and Excel software were used to calculate the statistics.

Image Preprocessing and Enhancement

The satellite images used in the study are Landsat 7 ETM+ (Collection 1, level 1), Landsat 8 OLI/TIRS (Collection 1, Level 1) satellite data belonging to the summer months of 2000, 2010, 2020 (Table 1). On May 31, 2003, a Scan Line Corrector (SLC) error occurred in its sensor on Landsat 7 ETM+ satellite images, resulting in approximately 22% data loss. Gaps were corrected by applying gap fill to Landsat 7 images of 2010 used in this study with the data accompanying the gap mask file (Yale, 2020). Images max. It is masked to have a cloud rate below 10%. Atmospherically corrected images were obtained geometrically ready.

NDVI-NDBI Index and LST Calculations

Land uses such as buildings, roads and industrial areas, parking lots are known as impermeable surfaces that can absorb short wave incoming solar radiation. Therefore, it has a direct impact on LST (Das et al., 2021). LST knowledge is essential for understanding different environmental changes. However, LST estimation becomes difficult due to the large number of land covers and surface heterogeneity caused by mixed land uses. Ecological parameters NDVI and NDBI are important to evaluate the change of LST.

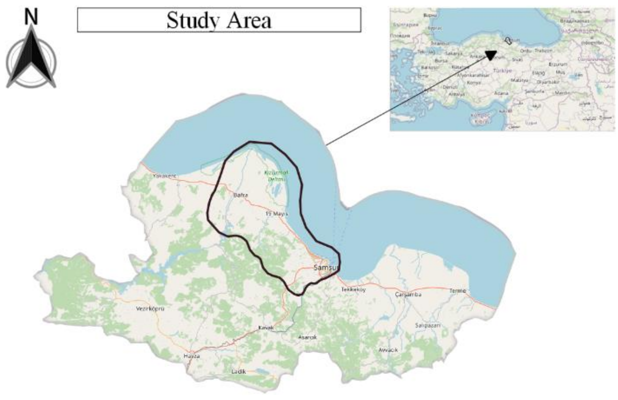

Figure 1. Study area

LST Formulas

Four known algorithms are used in LST calculations. These are Mono Window Algorithm (MWA) (Qin, Karnieli and Berliner, 2001), Single Channel Algorithm (SCA) (Jimenez-Munoz et al., 2009), (Mao et al., 2005; Yu et al. 2014).

Sekertekin and Bonafoni (2020) compared different algorithms used in LST calculations using Landsat 5,7,8 data in their study. According to the study, while MWA is applicable to all Landsat 5,7,8 data, it is only applicable to Landsat 8 OLI/TIRS data as SWA requires at least two TIR bands. Although TIRS bands are designed to allow the use of surface temperature acquisition algorithms, users are advised to avoid relying on band 11 data for quantitative analysis of TIRS data due to the calibration uncertainty associated with this band (Guha et al., 2018). For the study area, LST was taken from the 10th band of Landsat 7 ETM+ band 6, Landsat 8 OLI and TIRS image using the following algorithm (Artis and Carnahan, 1982).

- Calculation of TOA (Top of Atmospheric) spectral radiation

TOA (L) = M L × Q stay + A L (2)

ML = Band-specific multiplicative rescaling factor obtained from the metadata file (RADIANCE_MULT_BAND_ x where x is the band number).
Q cal = thermal band value
AL = Band-specific additive rescaling factor obtained from the metadata file (RADIANCE_ADD_BAND_ x where x is the band number).

- Convert from SSO to Luminosity Temperature (BT)

BT = (K 2 / (ln (K 1 / L) + 1)) - 273.15 (3)

K1 = Band-specific thermal conversion constant from metadata (K1_CONSTANT_BAND_ x where x is the thermal band number).
K2 = Band-specific thermal conversion constant from metadata (K2_CONSTANT_BAND_ x where x is the thermal band number).
L = TOA

- NDVI calculation

NDVI = (Nır – Red) / (Nır + Red) (4)

- Vegetation Pv rate calculation

P v = ((NDVI – NDVI min) / (NDVI max – NDVI min)) ² (5)

Surface emission, ε, was estimated using the NDVI thresholds method (Sobrino, Raissouni, & Li, 2001). The fractional vegetation of each pixel, Pv, was determined from NDVI using equation 6 (Carlson and Ripley, 1997).

- Emissivity calculation ε

ε = 0.004, * P v + 0.986 (6)

(Sobrino et al., 2001)

- Calculating Land Surface Temperature

LST = (BT / (1 + (0.00115 * BT / 1.4388) * Ln(ε))) (7)

(Weng and Yang, 2004)

Quantitative Analyzes

Land cover change was obtained from satellite images on the same dates with other parameters by using the maximum likelihood algorithm with controlled classification method. Land cover was evaluated in 4 classes. The classes within the study area were determined as (i) Water (River, Lake, Sea), (ii) Built up (Urban, Roads), (iii) Vegetation (Forest, Cropland, Delta, (iv) Open Land (Bare Soil) (Congedo, 2016).

$$r = \frac{\sum (x_i - \bar{x})(y_i - \bar{y})}{\sqrt{\sum (x_i - \bar{x})^2 \sum (y_i - \bar{y})^2}} \quad (8)$$

(Benesty et al., 2009)

Results

Land Cover Change Analysis Results

Table 2 shows the amount and rate of land change between 2000-2020. When the 20-year land change is examined, there has been a negligible change in the water surface at the borders of the study area. The significant change was experienced in green areas with a decrease of 14.1%. It is seen that this change in green areas is shared between bare soil and built areas at a rate of 7.33% and 7.1%. The Transition matrix numerically represents the different land cover forms that remain unchanged or change over the study periods.

Spatial Distribution and Evaluation Of LST, NDVI and NDBI

Table 3 contains descriptive statistical data for the entire study area. In Appendix 1, the LST thermal distribution map was created using appropriate color-coded ranges. (Oguz, 2013). When the maps in Appendix 1 are examined, it is observed that LST increases with the expansion in residential areas. It has been noticed that this increase is from urban centers to rural areas. The residential area on the Atakum coastline shows a tendency to expand by gradually moving away from the coast. In Bafra, on the other hand, the city center is located in the interior and it spreads radially. It is seen from the NDVI maps (Appendix 2) that the fields in Bafra have become more productive over the years with the fertile plain soils and the orientation to organic agriculture. Accordingly, enlargement in residential areas is associated with higher LST, lower NDVI. Declining NDVI can be attributed in part to established area expansion causing loss of vegetation and wetland cover. Also, Low NDVI denotes empty, uncultivated land areas. In order to better analyze the expansion of residential areas, NDVI and NDBI parameters were evaluated together. NDVI distribution maps are shown in Annex 2 and NDBI distribution maps in Annex 3. Max. While an increase of 1.69 C° is observed in LST from 2000 to 2020, there is no change in the average LST value. Heterogeneity is observed in the LST due to the variation of LU-LC dynamics in urban districts and rural districts within the study area. According to Table 3, the average NDVI value for the years 2000-2020 was 0.17 and 0.22, while the average NDBI value was 0.09 and -0.09.

Table 1. Satellite images used in the study

stellate	WRS-2 Row/Column	Date history	ID	Bands/Wavelength Spectral range (µm)	Resolution (m)
Landsat 7 ETM+	175/31	31.07.2000	LE07-L1TP-175031	band 3/ 0.630 -0.690 red 30	30
				Band 4/ 0.750 -0.900 Near Infrared 30	30
		12.08.2010	LE07-L1TP-175031	Band 5/ 1.55 -1.75 Shortwave Infrared	30
				Band 6/ 10.4-12.3 Thermal	60
Landsat 8 OLI/TIRS		25.06.2013	LC08-L1SP-175031	Band 4/ 0.64 –0.67 red 30	30
				Band 5/ 0.85 –0.88 Near Infrared (NIR) 30	30
		31.08.2020	LC08-L1SP-175031	Band 6/ 1.57 –1.65 Near Infrared (SWIR1	30
				Band 10 / 10.3-11.3 Thermal	100

Table 2. Change in land classes between 2000-2020

2000-2020							
Class Statistics							
Number	Class color	2000	2020	Δ	2000%	2020%	Δ %
1	Water	462.16 sq. km.	455.43 sq. km.	-6.73 sq. km.	23.71	23.37	-0.34
2	Built up	159.16 sq. km.	297.69 sq. km.	138.54 sq. km.	8.16	15.27	7.1
3	Vegetation	980.05 sq. km.	705.30 sq. km.	-274.75 sq. km.	50.29	36.19	-14.1
4	Open land	347.19 sq. km.	490.14 sq. km.	142.95 sq. km.	17.81	25.15	7.33
Transition Matrix							
Number	1	2	3	4			
1	0.96064	0.033146	0.004833	0.001381			
2	0.029892	0.479261	0.192231	0.298616			
3	0.006073	0.113058	0.622179	0.258691			
4	0.002157	0.274467	0.180607	0.542769			

Table 3. Descriptive statistical data for the entire study area

Evaluation	31.07.2000		12.08.2010		31.08.2020	
	Min.	Max.	Min.	Max.	Min.	Max.
LST (C°)	19.09	41.75	19.09	41.26	18.16	43.44
Mean	28.61		27.97		27.93	
Stad. Dev.	4.1		3.28		4.98	
NDVI	-0.43	0.49	-0.53	0.6	-0.18	0.63
Mean	0.17		0.21		0.22	
Stad. Dev.	0.13		0.16		0.20	
NDBI	-0.38	0.53	-0.53	0.59	-0.53	0.32
Mean	0.09		0.02		-0.09	
Stad. Dev.	0.11		0.13		0.12	
Average Temp. (C°)	23.8		26.8		24.3	

When we look at the statistical data in the whole city, there is no big change in the average value of LST in the 20-year period from 2000 to 2020, while max. It is seen that there is a 2°C increase in the LST value. For this reason, it was deemed appropriate to apply zonal statistical analysis in order to analyze the urban and rural districts separately.

Examining the Relationship Between LST and NDVI-NDBI on a County Basis

In order to analyze the NDVI-NDBI on the basis of urban and rural districts within the study area, district borders were cut from both parameter maps and a quantitative table was made (Table 4).

Average LST data did not vary greatly over the years, mean. NDVI has increased over the years, avg. NDBI, on the other hand, decreased. The change in NDVI and NDBI is not enough to affect the LST value. When the average LST data are analyzed on a district basis, Ilkadım and Atakum urban districts showed higher values. Cover. NDVI was found to be high in 19 May and Bafra, which are rural districts.

Statistical Verification of LST and NDVI-NDBI Data on a County Basis

It is known in the literature that looking at Table 5, the change in the R^2 correlation coefficient according to the districts of the years 2000, 2010, 2020 is seen. The results were found in accordance with the literature.

There is a strong inverse correlation between LST and NDVI for all three years. However, it is seen that the correlation coefficient is stronger in Ilkadım and Atakum urban districts. Correlation coefficient decreases in 19 Mayıs and Bafra rural districts. This is due to the existence of more heterogeneous landscapes within the residential area.

Table 4. LST, NDVI, NDBI descriptive data by districts

District	LST (C°)				NDVI				NDBI			
31/07/2000												
	Min	Max	Mean	StD	Min	Max	Mean	StD	Min	Max	Mean	StD
İlkadım	22.55	41.75	32.72	2.66	-0.47	0.44	0.19	0.08	-0.16	0.53	0.17	0.10
Atakum	21.70	40.52	30.22	3.38	-0.04	0.49	0.26	0.10	-0.21	0.44	0.09	0.12
19 Mayıs	19.97	39.28	29.74	2.75	-0.43	0.49	0.24	0.10	-0.37	0.46	0.11	0.11
Bafra	20.84	38.53	29.96	2.79	-0.07	0.46	0.21	0.09	-0.38	0.41	0.10	0.13
12.08.2010												
	Min	Max	Mean	StD	Min	Max	Mean	StD	Min	Max	Mean	StD
İlkadım	24.52	41.26	32.02	2.72	-0.12	0.53	0.21	0.10	-0.21	0.51	0.17	0.11
Atakum	21.41	38.53	28.83	3.58	-0.07	0.55	0.28	0.12	-0.33	0.47	0.06	0.13
19 Mayıs	22.27	36.25	28.17	2.34	-0.09	0.54	0.28	0.11	-0.53	0.46	0.02	0.11
Bafra	19.97	38.28	28.70	2.59	-0.11	0.55	0.27	0.13	-0.53	0.50	0.01	0.14
31.08.2020												
	Min	Max	Mean	StD	Min	Max	Mean	StD	Min	Max	Mean	StD
İlkadım	22.58	43.12	31.95	3.47	-0.18	0.58	0.24	0.11	-0.37	0.25	-0.04	0.10
Atakum	21.30	39.10	29.22	4.22	-0.13	0.61	0.32	0.14	-0.38	0.29	-0.11	0.12
19 Mayıs	22.11	38.67	29.45	3.43	-0.14	0.60	0.31	0.13	-0.42	0.26	-0.10	0.11
Bafra	19.51	42.95	29.64	4.29	-0.16	0.60	0.31	0.15	-0.51	0.18	-0.12	0.13

Table 5. Correlation equations and coefficients between LST- NDVI and LST- NDBI for districts

District	LST (C°)- NDVI		LST (C°)- NDBI	
31/07/2000				
	Denklem	Katsayı (R^2)	Denklem	Katsayı (R^2)
İlkadım	y=-18.603x+36.305	0.35	y=18.739x+29.378	0.55
Atakum	y=-21.994x+36.031	0.47	y=21.836x+28.054	0.61
19 Mayıs	y=-9.1062x+32.129	0.11	y=16.372x+28.071	0.51
Bafra	y=-8.4487x+31.649	0.08	y=15.448x+28.146	0.53
12.08.2010				
	Denklem	Katsayı (R^2)	Denklem	Katsayı (R^2)
İlkadım	y=-16.614x+35.468	0.40	y=18.876x+28.63	0.67
Atakum	y=-21.932x+35.202	0.62	y=23.482x+27.26	0.77
19 Mayıs	y=-7.9725x+30.507	0.17	y=15.485x+27.847	0.59
Bafra	y=-6.1449x+30.313	0.10	y=14.971x+28.376	0.64
31.08.2020				
	Denklem	Katsayı (R^2)	Denklem	Katsayı (R^2)
İlkadım	y=-17.369x+36.143	0.35	Y=23.802x+32.955	0.50
Atakum	y=-22.129x+36.548	0.57	Y=28.914x+32.482	0.70
19 Mayıs	y=-8.819x+32.229	0.14	Y=20.017x+31.526	0.50
Bafra	y=-12.285x+33.446	0.18	Y=21.88x+32.255	0.57

The increase in urbanization and impermeable surfaces cause different effects. The wider and holistic spread of fields and forest areas in rural districts decreases the correlation coefficient. It is obvious that apart from the variation between the districts, there has not been a big change between the years. In fact, by 2020, the NDVI value in Bafra district increased by 0.10. Therefore, the NDBI value also tends to decrease (Table 4). However, it is seen that the correlation is strong in Ilkadım and Atakum districts. Correlation coefficient decreases in 19 Mayıs and Bafra rural districts. (Table 5). This result informs LST that the effect of NDBI is greater. In other words, the effect of construction density on LST is more than the effect of green area density.

Discussions and Conclusion

In this article, the effect of NDVI and NDBI indexes on LST values of central districts Ilkadım and Atakum, rural districts 19 Mayıs and Bafra districts along the coastline of Samsun province were investigated. In order to investigate the LST density effect and to interpret the dynamic relationship between LST and NDVI and NDBI from the past to the present, the data of Landsat 8 OLI and TIRS and Landsat 7 ETM+ satellite images from 2000, 2010, 2020, which coincide with the month of August, were used. Care has been taken to ensure that the images coincide with the same month and are selected according to the cloudlessness filter. The study area was generally evaluated in terms of LU/LC classes (Built-up, Vegetation, Water, Bare soil).

The decrease in green space over the years has been revealed. In the light of recent studies, it has been revealed that bare soil areas, rocky areas and built-up areas affect LST in an upward direction, while wet areas and green areas have a decreasing effect on the contrary (Alademomi 2022; Alademomi 2020; Kulsum and Moniruzzaman 2022).; Ghouri et al. 2022; Khalis et al. 2021). A decrease of 14.1% was observed in the amount of green space throughout the study area in a 20-year period, while an increase was observed in open land and built-up classes (Table 2). In future studies, it is planned to analyze the land cover change by separating it on the basis of districts.

According to the results in Table 5, it is seen that the correlation between LST and NDVI is weaker than the correlation between LST and NDBI. This result informs LST that the effect of NDBI is greater. In other words, the effect of construction density on LST is more than the effect of green area density. In preventing the increase in LST in cities, preventing the increase of impermeable surfaces will have a great effect. Impervious surface reduction in urban landscape planning is important in controlling land surface temperature.

Many additional studies may be included in this study in the future. the work can be strengthened by calibrating and verifying the LST data with field measurements. Third, LST-NDVI/NDBI statistical evaluation can be made by separating the LU/LC classes of each district. New statistical methods can be applied in correlation estimation. Finally, the ecological assessment of the districts can be analyzed by incorporating more biophysical parameters.

Acknowledgements

As authors, I would like to thank my Ph.D. advisor of Kastamonu University and her advisory is Assoc. Prof. Dr. Mehmet Cetin for their support and assistance. This research has been produced from a part of Burcu Çevik Değerli's Ph.D. dissertation in Kastamonu University, Institute of Science, and Department of Landscape Architecture.

References

AK, 2013. Atakum Kaymakamlığı (AK). Değişirken, Gelişen Atakum. Available from https://www.atakum.gov.tr. [Accessed 05 June 2022].

Akinbobola A. 2019. Simulating land cover changes and their impacts on land surface temperature in Onitsha, South East Nigeria. Atmospheric and Climate Sciences, 9(02): 243. https://doi.org/10.4236/acs.2019.92017

Akinyemi FO, Ikanyeng M, Muro J. 2019. Land cover change effects on land surface temperature trends in an African urbanizing dryland region. City and environment interactions, 4, 100029. https://doi.org/10.1016/j.cacint.2020.100029

AlAdemomi AS, Okolie CJ, Daramola OE, Agboola RO, Salami TJ. 2020. Assessing the relationship of LST, NDVI and EVI with land cover changes in the Lagos Lagoon environment. Quaestiones Geographicae, 39(3): 87-109. https://doi.org/10.2478/quageo-2020-0025.

Alademomi AS, Okolie CJ, Daramola OE, Akinnusi SA, Adediran E, Olanrewaju HO, Odumosu J. 2022. The interrelationship between LST, NDVI, NDBI, and land cover change in a section of Lagos metropolis, Nigeria. Applied Geomatics, 14(2): 299-314. https://doi.org/10.1007/s12518-022-00434-2

Artis DA, Carnahan WH. 1982. Survey of emissivity variability in thermography of urban areas. Remote Sensing of Environment, 12(4): 313-329. https://doi.org/10.1016/0034-4257(82)90043-8

Bağci H, Bahadır M. 2019. Land use and temporal change in Kızılırmak Delta (Samsun) (1987-2019). Journal of Academic Social Science Studies (78): 295-312. doi.10.9761/JASSS40162

Benesty J, Chen J, Huang Y, Cohen I. 2009. Pearson Correlation Coefficient. In: Noise Reduction in Speech Processing. Springer Topics in Signal Processing, vol 2. Springer, Berlin, Heidelberg. https://doi.org/10.1007/978-3-642-00296-0_5

Carlson TN, Ripley DA. 1997. On the relation between NDVI, fractional vegetation cover, and leaf area index. Remote Sensing of Environment, 62(3): 241-252. doi: https://doi.org/10.1016/S0034-4257(97)00104-1.

Change IC. 2019. Land: An IPCC Special Report on Climate Change. Desertification, Land Degradation, Sustainable Land Management, Food Security, and Greenhouse Gas Fluxes in Terrestrial Ecosystems, 1-864.

Congedo L. 2016. Semi-Automatic Classification Plugin: A Python tool for the download and processing of remote sensing images in QGIS. Journal of Open-Source Software, 6(64): 3172, https://doi.org/10.21105

Çelik B. 2019. Arazi örtüsü değişimlerinin kentsel ısı adalarına olan etkilerinin zamansal ve mekansal olarak araştırılması (Spatio-temporal analyses of land cover changes and its impacts on urban heat islands). İstanbul Teknik Üniversitesi, Fen Bilimleri Enstitüsü, Doktora Tezi (PhD.), 140 s., İstanbul, Türkiye. (In Turkish)

Das N, Mondal P, Sutradhar S, Ghosh R. 2021. Assessment of variation of land use/landcover and its impact on land surface temperature of Asansol subdivision. The Egyptian Journal of Remote Sensing and Space Science, 24(1): 131-149. https://doi.org/10.1016/j.ejrs.2020.05.001

Guha S, Govil H, Dey A, Gill N. 2018. Analytical study of land surface temperature with NDVI and NDBI using Landsat 8 OLI and TIRS data in Florence and Naples city, Italy. European Journal of Remote Sensing, 51(1): 667-678. https://doi.org/10.1080/22797254.2018.1474494

Ghouri AY, Khan A, Rasheed F. 2022). Monitoring The Land Surface Temperature and Its Correlation with NDVI of Chiniot by Using GIS Technology and Remote Sensing. Eart and Envi Scie Res & Rev. 5(2): 01, 9. https://doi.org/10.21203/rs.3.rs-1468097/v1

Guler M, Cemek B, Gunal H. 2007. Assessment of some spatial climatic layers through GIS and statistical analysis techniques in Samsun Turkey. Meteorological Applications: A journal of forecasting, practical applications, training techniques and modelling, 14(2): 163-169. https://doi.org/10.1002/met.18

Jimenez-Munoz JC, Cristobal J, Sobrino JA, Soria G, Ninyerola M, Pons X. 2009. Revision of the Single-Channel Algorithm for Land Surface Temperature Retrieval from Landsat Thermal-Infrared Data. IEEE Transactions on Geoscience and Remote Sensing, 47(1): 339-349. doi:10.1109/TGRS.2008.2007125

Karabulut M, Gürbüz M, Korkmaz H. 2008. Precipitation and temperature trend analyses in Samsun. Journal International Environmental Application & Science, 3(5): 399-408.

Khalis H, Sadiki A, Jawhari F, Mesrar H, Azab E, Gobouri AA, Bourhia M. 2021. Effects of Climate Change on Vegetation Cover in the Oued Lahdar Watershed. Northeastern Morocco. Plants, 10(8): 1624. https://doi.org/10.3390/plants10081624

Kulsum U, Moniruzzaman M. 2022. Exploring the relationship of climate change and land-use dynamics with satellite-derived surface indices and temperature in greater Dhaka, Bangladesh. Journal of Earth System Science, 131(2): 1-15. https://doi.org/10.1007/s12040-022-01841-0

Mao K, Qin Z, Shi J, Gong P. 2005. A practical split-window algorithm for retrieving land-surface temperature from MODIS data. International Journal of Remote Sensing, 26(15): 3181-3204. doi:10.1080/01431160500044713

Oguz H. 2013. LST calculator: A program for retrieving land surface temperature from Landsat TM/ETM+ imagery. Environmental Engineering and Management Journal, 12(3): 549-555.

Oke TR. 1982. The energetic basis of the urban heat island. Quarterly Journal of the Royal Meteorological Society, 108(455): 1-24.

Oleson KW, Bonan GB, Feddema J, Jackson T. 2011. An examination of urban heat island characteristics in a global climate model. International Journal of Climatology, 31(12): 1848-1865. https://doi.org/10.1002/joc.2201

Ozturk D. 2017. Assessment of urban sprawl using Shannon's entropy and fractal analysis: a case study of Atakum, Ilkadim and Canik (Samsun, Turkey). Journal of environmental engineering and landscape management, 25(3): 264-276. https://doi.org/10.3846/16486897.2016.1233881

Pielke Sr RA. 2005. Land use and climate change. Science, 310(5754): 1625-1626. doi: 10.1126/science.1120529

Qin Z, Karnieli A, Berliner P. 2001. A mono-window algorithm for retrieving land surface temperature from Landsat TM data and its application to the Israel-Egypt border region. International Journal of Remote Sensing, 22(18): 3719-3746. doi:10.1080/01431160010006971

Roth M. 2007. Review of urban climate research in (sub) tropical regions. International Journal of Climatology: A Journal of the Royal Meteorological Society, 27(14): 1859-1873. https://doi.org/10.1002/joc.1591

SBB, 2014. Samsun Büyükşehir Belediyesi (SBB). 2014 raporu. 2015-2019 Stratejik Planı. Available from https://samsun.bel.tr. [Accessed 06 June 2021].

Sekertekin A, Bonafoni S. 2020. Land surface temperature retrieval from Landsat 5, 7, and 8 over rural areas: assessment of different retrieval algorithms and emissivity models and toolbox implementation. Remote Sensing, 12(2): 294. https://doi.org/10.3390/rs12020294

SİTOM, 2007. Samsun İl Tarım ve Orman Müdürlüğü (SİTOM). Samsun İlinin Fiziki Durumu ve Avantajları. Available from https://samsun.tarimorman.gov.tr [Accessed 01 July 2022].

SKTM, 2020. Samsun İl Kültür ve Turizm Müdürlüğü (SKTM). Available from: https://samsun.ktb.gov.tr/ [Accessed 10.04.2020].

Sobrino JA, Raissouni N, Li ZL. 2001. A Comparative Study of Land Surface Emissivity Retrieval from NOAA Data. Remote Sensing of Environment, 75(2): 256-266. doi: https://doi.org/10.1016/S0034-4257(00)00171-1

TÜİK, 2020. Türkiye İstatistik Kurumu (TÜİK). İstatistik göstergeler. Available from https://data.tuik.gov.tr/Bulten/Adrese-Dayali-Nufus-Kayit-Sistemi-Sonuclari-2020-37210 [Accessed 02 May 2021].

USGS, 2020. United States Geological Survey (USGS). Earth Explorer. Available from https://earthexplorer.usgs.gov/ [Accessed on 10 January 2020].

Ülke A, Özkoca T. 2018. Sinop, Ordu ve Samsun illerinin sıcaklık verilerinde trend analizi. (Trend Analyses of Temperature Data of Sinop, Ordu and Samsun Provinces) Gümüşhane Üniversitesi Fen Bilimleri Dergisi, 8(2): 455-463. (ın Turkish) https://doi.org/10.17714/gumusfenbil.351294

Weng Q, Yang S. 2004. Managing the adverse thermal effects of urban development in a densely populated Chinese city. Journal of Environmental management, 70(2): 145-156. https://doi.org/10.1016/j.jenvman.2003.11.006

Yale 2020. Yale University. Center for Earth Observation. Landsat. Avaiable from https://yceo.yale.edu/ [Accessed 01.08.2020].

Yu X, Guo X, Wu Z. 2014. Land Surface Temperature Retrieval from Landsat 8 TIRS—Comparison between Radiative Transfer Equation-Based Method, Split Window Algorithm and Single Channel Method. Remote Sensing, 6(10). doi:10.3390/rs6109829